Subcellular properties of triggered Ca^{2+} waves in isolated citrate-loaded guinea-pig atrial myocytes characterized by ratiometric confocal microscopy

Peter Lipp*, Jörg Hüser†, Lutz Pott‡ and Ernst Niggli

Department of Physiology, University of Bern, CH-3012 Bern, Switzerland, †Institute for Cell Physiology and ‡Department of Physiology, Ruhr-University Bochum, D-44780 Bochum, Germany

1. Spatiotemporal aspects of subcellular Ca^{2+} signalling were studied in cultured adult guinea-pig atrial myocytes. A mixture of the Ca^{2+} indicators fluo-3 and Fura Red in combination with laser-scanning confocal microscopy was used for $[Ca^{2+}]_i$ measurements while membrane currents were recorded simultaneously.

2. In citrate-loaded atrial myocytes not every Ca^{2+} current (I_{Ca}) could trigger Ca^{2+} release from the sarcoplasmic reticulum (SR). Two types of Ca^{2+} signals could be observed: Ca^{2+} transients resulting from (i) Ca^{2+} influx alone and (ii) additional Ca^{2+} release.

3. Ca^{2+} release elicited by voltage steps of 100–150 ms duration was either apparently homogeneous or propagated as Ca^{2+} waves through the entire cell. With brief I_{Ca} (50–75 ms), Ca^{2+} waves with limited subcellular propagation were observed frequently. These waves always originated from either end of the myocyte.

4. The time course of changes in Na^+–Ca^{2+} exchange current (I_{NaCa}) depended on the subcellular properties of the underlying Ca^{2+} transient and on the particular cell geometry. Apparently homogeneous Ca^{2+} release was accompanied by an inward change of I_{NaCa} the onset phase of which was fused with I_{Ca}. Changes in I_{NaCa} caused by a Ca^{2+} wave propagating through the entire cell showed a W shape, which could be attributed to differences of the fractional surface-to-volume ratio in different cell segments during propagation of the Ca^{2+} wavefront. Those waves with limited spreading only activated a small component of I_{NaCa}.

5. The different subcellular patterns of Ca^{2+} release signals can be explained by spatial inhomogeneities in the positive feedback of the SR. This depends on the local SR Ca^{2+} loading state under the control of the local Ca^{2+} influx during activation of I_{Ca}. Due to the higher surface-to-volume ratio at the two ends of the myocyte, SR loading and therefore the positive feedback in Ca^{2+}-induced Ca^{2+} release may be higher at the ends, locations where Ca^{2+} waves are preferentially triggered.

6. We conclude that the individual cell geometry may be an important determinant of subcellular Ca^{2+} signalling not only in cardiac muscle cells but presumably also in other types of cells that depend on Ca^{2+} signalling. In addition, the cell geometry in combination with varying subcellular Ca^{2+} release patterns can greatly affect the time course of Ca^{2+}-activated membrane currents.

The release of Ca^{2+} ions from the sarcoplasmic reticulum (SR) is the principal link between the electrical excitation of the plasma membrane and the mechanical activity of mammalian cardiac myocytes. It is generally accepted that Ca^{2+} release from the SR by a mechanism referred to as 'Ca^{2+}-induced Ca^{2+} release' (CICR) is triggered via Ca^{2+} influx across the plasma membrane (for a review see Callewaert, 1992). Two pathways are known for this Ca^{2+} influx: (i) L-type Ca^{2+} channels and (ii) reverse-mode Na^+–Ca^{2+} exchange (Lipp & Niggli, 1994*a*; for reviews see Callewaert, 1992; Niggli & Lipp, 1995).

* To whom correspondence should be addressed at The Babraham Institute, Babraham Hall, Babraham, Cambridge CB2 4AT, UK.

The complex morphology of the Ca^{2+} signalling apparatus in cardiac muscle cells supports the notion that the function of excitation–contraction coupling (E–C coupling) critically depends on the ultrastructural arrangement of the contributing signalling components (i.e. sarcolemmal and sarcoplasmic membranes with associated proteins). Ca^{2+} imaging studies (Takamatsu & Wier, 1990) indicated that in cardiac ventricular myocytes Ca^{2+} release from the SR triggered by an action potential or a voltage-clamp depolarization is spatially homogeneous (see also Cheng, Lederer & Cannell, 1994). Ventricular myocytes are known to possess a well-developed t-tubular system which ensures the spreading of the electrical excitation into the cell interior. Moreover, terminal SR cisternae are in close contact with the t-tubular membrane forming diads or triads (Sommer & Jennings, 1986). Thus, the ultrastructure of the ventricular myocyte favours subcellularly uniform Ca^{2+} release from the SR.

In contrast, atrial myocytes lack a t-tubular system and except of peripheral couplings between the SR and the sarcolemmal membrane a large fraction of the SR does not exhibit coupling to the surface membrane (e.g. corbular SR; Sommer & Jennings, 1986). In isolated atrial myocytes, the analysis of Ca^{2+} release-dependent transient inward currents (referred to as I_{NaCa}), reflecting Ca^{2+} extrusion via Na^+–Ca^{2+} exchange, revealed two distinct current components (Budde, Lipp & Pott, 1991). This observation was interpreted as reflecting two functionally distinct SR compartments with different properties of Ca^{2+} release (Lipp, Pott, Callewaert & Carmeliet, 1990). Furthermore, it was proposed that these two current components reflect Ca^{2+} release from a peripheral and a central SR compartment. SR Ca^{2+} release from the superficial compartment would result in small but rapid membrane current components while release from the central compartment generated large but slower inward shifts of I_{NaCa} (large current component). A detailed comparison of I_{NaCa} as an indicator for the subsarcolemmal $[Ca^{2+}]$ and the whole-cell indo-1 fluorescence for the bulk $[Ca^{2+}]$ supported this hypothesis (Lipp *et al.* 1990). During the initial period of Ca^{2+} release the $[Ca^{2+}]$ calculated from the whole-cell indo-1 fluorescence was less than expected from simultaneously measured I_{NaCa}, while during the relaxation of the intracellular Ca^{2+} transient both $[Ca^{2+}]$ measurements indicated similar values for $[Ca^{2+}]_i$ (Lipp *et al.* 1990). These experimental results were interpreted in terms of subsarcolemmal $[Ca^{2+}]$ gradients during the early period of signal transduction in atrial myocytes probably arising from initial Ca^{2+} release from a peripheral SR compartment. In addition, the proposed peripheral SR compartment was not only able to exhibit Ca^{2+} release but could also attenuate Ca^{2+} influx transients through voltage-operated Ca^{2+} channels (Lipp, Pott, Callewaert & Carmeliet, 1992). In a recent study on field-stimulated cat atrial myocytes some evidence for a similar mechanism has been presented (Hüser, Lipsius & Blatter, 1996). By means of confocal microscopy the authors provided experimental evidence showing that SR Ca^{2+} release in atrial myocytes lacking t-tubules propagated from the surface of the cell into deeper cell layers. When field-stimulating cat atrial myocytes were loaded with the acetoxymethyl ester form of fluo-3 (fluo-3 AM), Ca^{2+} release was preferentially initiated at locations underneath the cell membrane and subsequently invaded the deeper cell interior. A similar process has been suggested recently in E–C coupling in rat ventricular myocytes (Trafford, Diaz, O'Neill & Eisner, 1995*a*).

In the present study, cultured guinea-pig atrial myocytes were studied using a combination of ratiometric confocal microscopy and whole-cell patch clamp recording to investigate the possible effect of the cell geometry on subcellular aspects of SR Ca^{2+} release and the time course of I_{NaCa}. Preliminary results have been presented (Hüser, Lipp, Pott & Niggli, 1994).

METHODS

Cell isolation and culture

Guinea-pig atrial myocytes were isolated and cultured according to established methods (Bechem, Pieper & Pott, 1985). In brief, adult guinea-pigs (weight, 200–300 g) of either sex were killed by cervical dislocation after stunning. The hearts were removed quickly and single cells were isolated using standard enzymatic procedures. The cell suspension was transferred onto glass coverslips at a final density of about 1000 cells per coverslip. They were placed into multiwell culture dishes and stored in an incubator at 37 °C (100% humidity, 2% CO_2).

Solutions

The cells were kept in a culture medium based on M199 (Gibco) with added gentamicin (0·1 mg (100 ml)$^{-1}$; ICN Biomedicals, Costa Mesa, CA, USA) and fetal calf serum (10%; Boehringer Mannheim). The regular extracellular medium during the experiments contained (mM): 135 NaCl, 4 KCl, 2 $CaCl_2$, 2 $MgCl_2$, 10 glucose, 10 Hepes; adjusted to pH 7·4 with NaOH. The pipette solution for internal dialysis of the single atrial myocytes contained (mM): 65 caesium citrate, 10 CsCl, 10 NaCl, 1 $MgCl_2$, 5 MgATP, 0·04 $(NH_4)_5$fluo-3, 0·08 $(NH_4)_4$Fura Red (both from Molecular Probes Inc., Eugene, OR, USA), 10 Hepes; adjusted to pH 7·2 with CsOH. All experiments were carried out at room temperature (20–22 °C).

Current measurement

Prior to the experiments the coverslips with the attached cells were placed in a sandwich chamber on an inverted microscope (TMD Diaphot; Nikon, Tokyo, Japan) and the culture medium was replaced with the extracellular solution. Membrane currents were measured in the whole-cell configuration of the patch clamp technique. Patch clamp electrodes were pulled from filamented glass pipettes (GC150F; Clark Electromedical Instruments, Reading, UK) on a horizontal puller (BB-CH; Mecanex, Geneva, Switzerland) to a final resistance ranging from 1 to 2 MΩ. The membrane voltage was controlled by a patch clamp amplifier (Axon Instruments). Membrane potentials and currents were recorded using custom-made software developed with LabView software (National Instruments, Austin, TX, USA) on a Macintosh IIcx computer (Apple, Wallisellen, Switzerland) equipped with a data acquisition board (MIO-16 H9; National Instruments, Austin, TX, USA).

$[Ca^{2+}]_i$ measurements

Spatial aspects of intracellular Ca^{2+} transients in the cardiac myocytes were investigated using a laser-scanning confocal

microscope (Lipp & Niggli, 1993). In brief, the set-up was based on a confocal laser-scanning head stage (MRC-600; BioRad, Wetzikon, Switzerland) attached to an inverted microscope. A mixture of two Ca^{2+} indicators, fluo-3 (F3) and Fura Red (FR), was used to obtain ratiometric [Ca^{2+}] measurements as described by Lipp & Niggli (1993). For excitation of the Ca^{2+} indicators the 514 nm line of the argon ion laser was used. Emission was collected at 540 ± 15 nm (F3) and > 600 nm (FR). The set-up was mounted on top of an air-driven vibration-isolated table and was shielded by a Faraday cage. For confocal image sequences a small window (192 pixels × 192 pixels) was chosen and repetitively scanned with a maximal frequency of 8 Hz. The resulting images were simultaneously recorded with an S-VHS video recorder (VHR-6850H HQ; Sony). For analysis of the sequences each frame was digitized by a frame-grabber card (RasterOps 24-STV) running on a Macintosh IIcx computer. The fluorescence ratio was obtained by dividing the fluo-3 and Fura Red images pixel by pixel. For a higher temporal resolution the linescan mode of the confocal microscope was used (Lipp & Niggli, 1993). The confocal images were initially stored on a magneto-optical drive (APS 128 MO; APS Technologies, MO, USA) and later transferred to digital audiotape (Turbo-DAT; APS Technologies) for long-term storage. The image analysis was performed with a modified version of the image-processing software 'NIH-Image' running on a Macintosh IIcx computer.

RESULTS

Ca^{2+} signals during a train of I_{Ca} visualized by confocal image sequences

Temporal and spatial aspects of subcellular Ca^{2+} signals in atrial myocytes were investigated using trains of step depolarizations from a holding potential of −50 mV to +5 mV (duration, 150 ms; frequency, 0·5–1·5 Hz). Figure 1 shows representative results obtained from a citrate-loaded myocyte. The presence of citrate caused a separation of the Ca^{2+} signals into transients representing pure Ca^{2+} influx and those reflecting additional triggered SR Ca^{2+} release (see Lipp *et al.* 1990). SR Ca^{2+} release was evident as an inward current carried by forward-mode Na^+–Ca^{2+} exchange after activation of I_{Ca}, which serves as the Ca^{2+} trigger signal via CICR. No spontaneous SR Ca^{2+} release was observed under these conditions ($n = 20$ cells).

In this sequence two of the I_{Ca} were followed by an inward change in I_{NaCa}. A comparison of the two signals revealed pronounced differences in their time courses. While the initial phase of the first I_{NaCa} was fused with I_{Ca}, a dissociation between I_{NaCa} and I_{Ca} and two components were evident in the second inward current. Simultaneously acquired confocal sections from the atrial myocyte indicated that the properties of the inward currents were caused by the spatiotemporal characteristics of the underlying SR Ca^{2+} release (see Fig. 1*B* and *C*). Within the limited temporal resolution of ~125 ms per image, the rise and decline of the first Ca^{2+} transient were apparently homogeneous throughout the entire cell as evidenced by the confocal image sequence (Fig. 1*B*), while subcellular inhomogeneities could be observed during the second Ca^{2+} release signal (Fig. 1*C*). This Ca^{2+} transient originated from the lower left end and thereafter spread longitudinally through the myocyte, characteristics that identified the transient as a subcellular Ca^{2+} wave (Lipp & Niggli, 1993*a*, 1994*b*). In contrast to the spontaneous Ca^{2+} waves described recently, the Ca^{2+} waves here were triggered by Ca^{2+} influx through L-type Ca^{2+} channels (I_{Ca}-triggered Ca^{2+} waves).

I_{Ca}-triggered Ca^{2+} waves were found in all cells examined under the present conditions ($n = 20$) and represent the first observation of Ca^{2+} waves induced by Ca^{2+} influx through voltage-operated channels in cardiac myocytes. Moreover, Fig. 1 provides strong evidence for an operating E–C coupling mechanism despite the presence of citrate, since a contraction of the myocyte is obvious from the confocal image sequence in Fig. 1*B* (notice the change of the cell shape; similar contractions were found in all cells).

Linescan image analysis of I_{Ca}-triggered Ca^{2+} signals

The recording of confocal sections provides a high spatial resolution but has the drawback of a limited temporal resolution (acquisition rate, ~8 Hz; see Methods). In the linescan mode of the confocal set-up one of the two spatial dimensions is sacrificed for a higher temporal resolution (for a detailed description of the linescan mode see Lipp & Niggli, 1993*a*). A single line from the entire confocal section is chosen, scanned repetitively and ordered sequentially to build up the linescan image. A representative example of such a recording is shown in Fig. 2. In order to record a complete depolarization train of ~20 s, we reduced the scanning rate to 25 Hz since the maximum number of repetitive scans from the same line was restricted to 512 with our confocal microscope. Again in this example only two I_{Ca} triggered Ca^{2+} release. Both Ca^{2+} transients were paralleled by a transient change in I_{NaCa} characterized by a biphasic initial phase. The simultaneously recorded linescan image (Fig. 2*E*) classified the underlying Ca^{2+} transient as a subcellular Ca^{2+} wave (see Lipp & Niggli, 1994*b*). In contrast to homogeneous Ca^{2+} signals, Ca^{2+} waves exhibited an increase in $[Ca^{2+}]_i$ that was not parallel to the scanned line (i.e. not simultaneous within a single line). This property was also found in the linescan image in Fig. 2*E*. To emphasize the propagation of the subcellular Ca^{2+} transient we averaged parts of the linescan image corresponding to the two ends of the cell (see Fig. 2*E*). Initially, the Ca^{2+} signal appeared in the lower half (Fig. 2*D*, marked in red) and propagated into the upper part of the cell (Fig. 2*D*, marked in green). It should be noted here that the Ca^{2+} release signal derived from the upper part of the myocyte was preceded by an influx transient while both transients were temporally fused in the transient averaged from the lower part of the cell. This observation indicates that the Ca^{2+} transient was triggered by I_{Ca} only in the lower part but not in the upper part of the myocyte. Despite a constant or even decreasing amplitude of I_{Ca} a positive staircase of the Ca^{2+} influx transients was visible, which was typical for the present experimental conditions. This phenomenon was attributed to an attenuation of the 'real' Ca^{2+} influx signal by the peripheral SR compartment (Lipp *et al.* 1992). All these properties taken together supported our interpretation

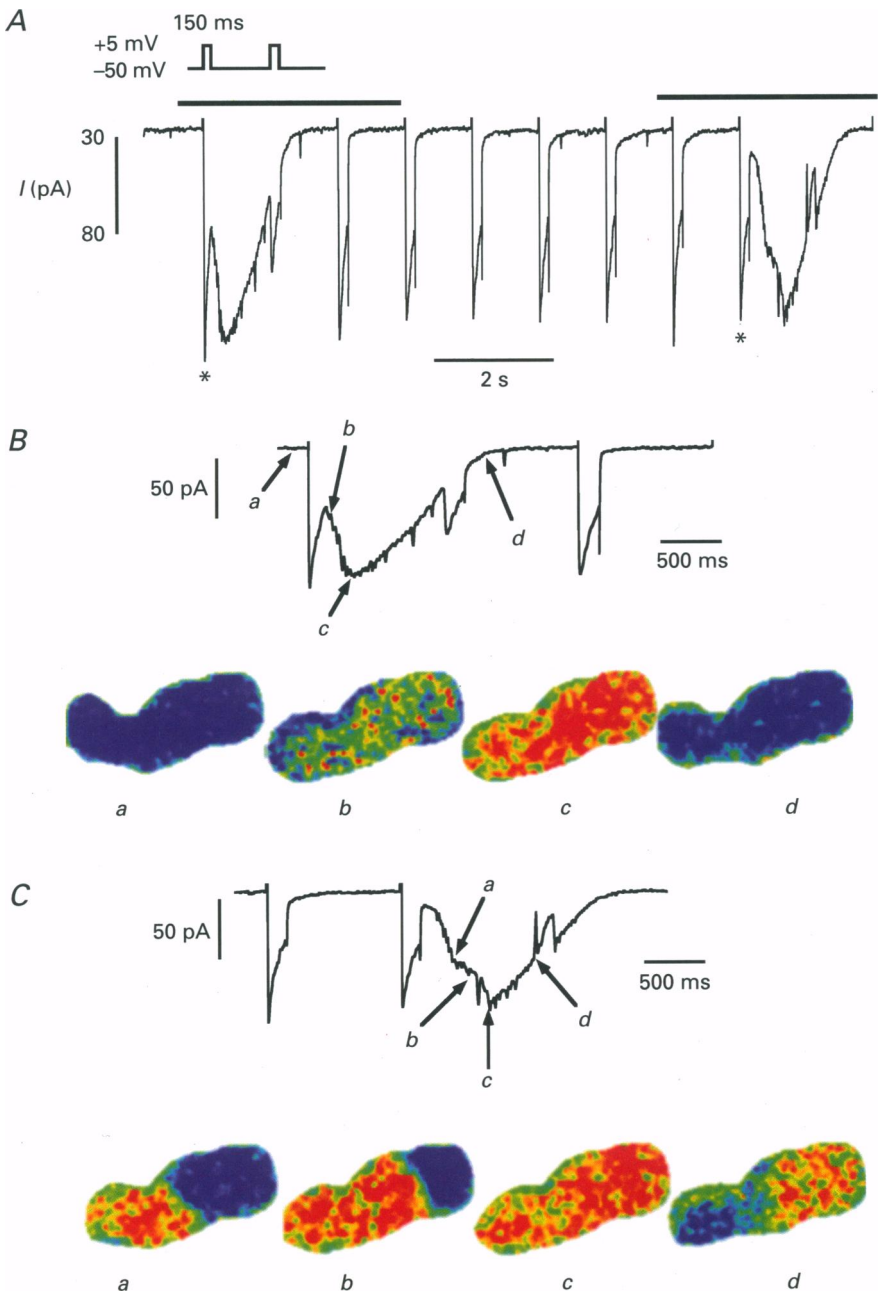

Figure 1. Sequences of ratiometric confocal sections during a train of I_{Ca} with long duration

A cultured guinea-pig atrial myocyte was voltage clamped at −50 mV and depolarizations to +5 mV were applied (duration, 150 ms; frequency, ~1 Hz) which elicited I_{Ca}. Due to the presence of a high concentration of the low-affinity Ca^{2+} buffer citrate only two I_{Ca}-triggered SR Ca^{2+} releases (*) were visible as transient inward shifts of I_{NaCa} (*A*). Simultaneously recorded ratiometric confocal images (*B* and *C*) revealed different subcellular properties for the two SR Ca^{2+} release signals. The first (*A*) was characterized by an upstroke phase of I_{NaCa} that was fused with I_{Ca}. The corresponding confocal sections (*B*, left-hand horizontal bar in *A*) showed a homogeneous Ca^{2+} release (at an acquisition rate of 8 Hz). The second current transient with a biphasic upstroke was caused by a subcellular Ca^{2+} wave as shown by the confocal sections in *C* (right-hand horizontal bar in *A*). For *B* and *C* the arrowheads and the characters in the current traces mark the time for the corresponding confocal sections. The rapid downward deflections of the membrane current in this and the following figures are due to the gating of a large conductance channel described previously (Pott & Mechmann, 1990).

that the biphasic current transients resulted from subcellular Ca^{2+} waves (similar biphasic current transients were found in all cells examined under similar conditions; $n = 20$).

In adult guinea-pig atrial myocytes I_{Ca} was the only source for Ca^{2+} influx since the Na^+–Ca^{2+} exchange was operating in its forward mode under the current experimental conditions. Therefore the loading state of the SR is mainly determined by I_{Ca}-mediated Ca^{2+} influx. Since I_{Ca} with long durations (i.e. 150 ms) caused propagating Ca^{2+} waves that have been attributed to a high degree of positive feedback in the CICR mechanism (see Niggli & Lipp, 1995), we reduced the Ca^{2+} load of the myocyte by decreasing the duration of I_{Ca} and thereby lowering Ca^{2+} influx in order to decrease the probability of Ca^{2+} wave propagation.

Brief depolarizations trigger Ca^{2+} release with limited spatial spreading

Trains of depolarizations $\leqslant$ 100 ms in duration to the same myocyte resulted in current recordings as shown in Fig. 3*A*. Again, two types of I_{NaCa} could be observed. These were a large component already described for Figs 1 and 2 and an additional small current component that followed the 4th, 5th, 7th and 8th I_{Ca}. Similar components of I_{NaCa} have already been described in atrial myocytes (Lipp *et al.* 1990) and were interpreted as a result of Ca^{2+} release from a subsarcolemmal SR compartment. However, the sequence of ratiometric confocal sections revealed a different feature of the subcellular Ca^{2+} signals (see Fig. 3*C*). As for the Ca^{2+} waves already described, the Ca^{2+} transients accompanying the small current components originated from one of the two ends of the cell but exhibited only a subcellulary limited propagation through the upper part of the cell (see representative confocal sequence in Fig. 3*C*). Propagation ceased in the middle of the cell. No SR Ca^{2+} release signal was detected in the lower part. Therefore we suggest that the small current components resulted from spatially restricted Ca^{2+} release (similar small components could be found in all cells investigated using appropriate depolarization protocols; $n = 12$).

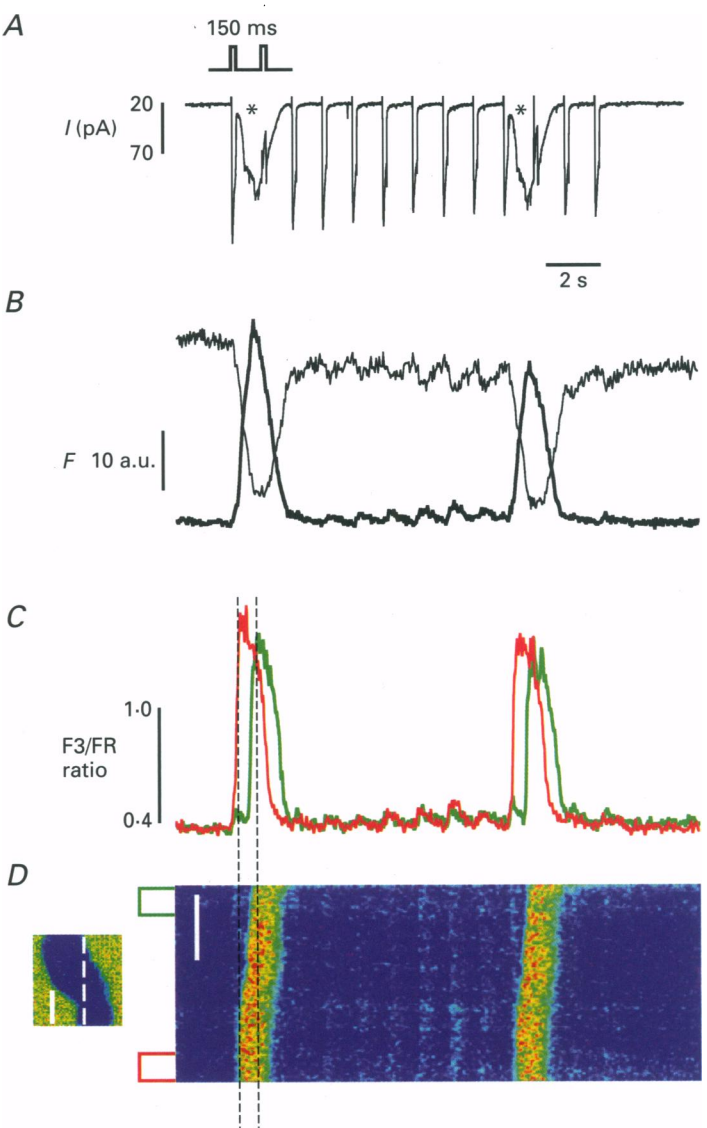

Figure 2. Linescan image recorded during a train of I_{Ca}

Current and fluorescence recordings from a myocyte voltage clamped at −50 mV and depolarized to +5 mV for 150 ms at a frequency of ~1 Hz. Two I_{Ca} were able to trigger SR Ca^{2+} release (* in *A*). *B* shows the simultaneous recordings of the fluo-3 (thick trace) and Fura Red (thin trace) in the linescan mode of the confocal microscope. For this mode a single line of the entire confocal image was chosen, repetitively scanned at a frequency of 25 Hz and arranged in a left–right order. Therefore time runs from left to right while the preserved spatial dimension is represented in the vertical direction. *C* shows the time course of the fluo-3/Fura Red (F3/FR) ratio averaged from the ratiometric linescan image in *D*. The colour coding in *C* identifies the two marked horizontal bars in the linescan image. The location of the chosen line (dashed line) is marked in the inset to the left of *D*, which shows an ratiometric confocal section through the atrial myocyte. Scale bar, 10 μm.

Two components in I_{NaCa} reflect SR Ca^{2+} release with limited subcellular propagation

A more distinct dissociation of the two current components was obtained by reducing the duration of the I_{Ca} even further (see Lipp *et al.* 1990; Budde *et al.* 1991). Figure 4 shows current and Ca^{2+} recordings from the same cell when step depolarizations were shortened to 75 ms. Not every I_{Ca} was able to induce Ca^{2+} release from the SR as evidenced by the lack of I_{NaCa}. Two small (following the 1st and the 7th depolarization) and a large sized inward current (triggered by the 4th I_{Ca}) were visible. While the two small components were characterized by a monophasic rising and declining phase the large current transient was clearly composed of two smaller components giving rise to the W shape described previously (Budde *et al.* 1991). To analyse the relation between the two small components and the large sized current the 'whole line' (i.e. averaged from the entire line chosen for this linescan) and local $[Ca^{2+}]$ transients and the shape of the I_{NaCa} time course were compared (see Fig. 4*E*).

All I_{NaCa} signals in this trace were a result of subcellular Ca^{2+} waves as revealed by the linescan image. The front of each of the transients was not parallel to the scanned line but instead showed a clear deviation. The second Ca^{2+} wave propagated through the entire cell while the subcellular properties of the

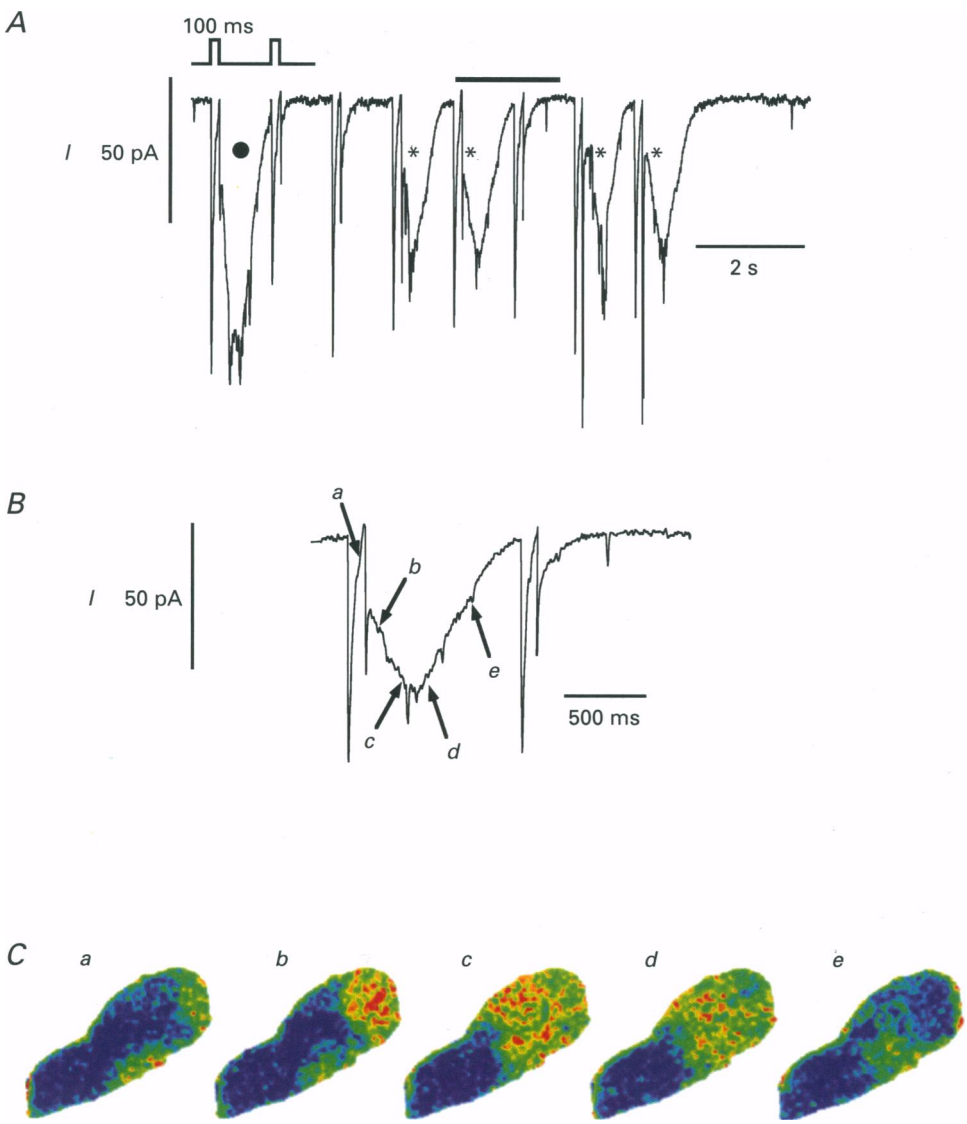

Figure 3. Membrane currents and ratiometric confocal sequence of a subcellular I_{Ca}-triggered Ca^{2+} wave with limited propagation

Current recording and ratiometric confocal sequence during a train of depolarizations from −50 mV to +5 mV (duration, 100 ms; frequency, ~1 Hz). The Ca^{2+} currents triggered SR Ca^{2+} release characterized by different time courses of the accompanying I_{NaCa}. A large current transient (●) and several small current components (*) were visible (*A*). Part of the current trace (marked with the horizontal bar) was reproduced in *B* at a higher temporal resolution. The simultaneously recorded ratiometric confocal sequence (*C*) characterized the underlying Ca^{2+} transient as a Ca^{2+} wave with spatially restricted propagation.

two other transients resembled characteristics of the Ca^{2+} wave shown in Fig. 3. The spreading of the Ca^{2+} transient was restricted to the lower half of the cell. Thus the two small current components may be due to spatially restricted Ca^{2+} release from only part of the cell.

If the spatial property of the subcellular Ca^{2+} release pattern determines the time course of the Na^{+}–Ca^{2+} exchange current, then current transients accompanying SR Ca^{2+} release events that occurred only in one of the two ends of the cell should match the time course of the local Ca^{2+}

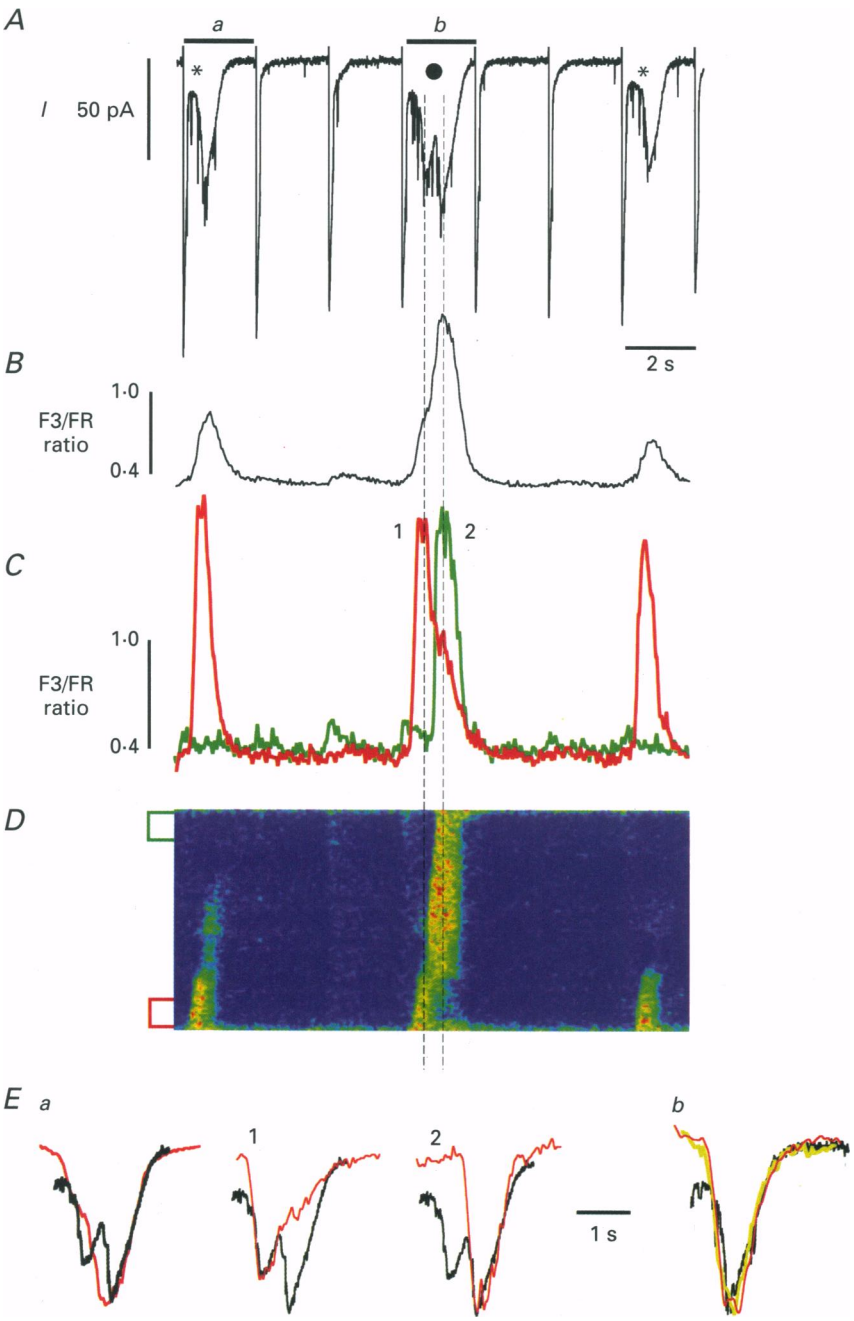

Figure 4. Linescan image and current recordings during a train of short I_{Ca}

Current recordings and ratiometric linescan image during a train of depolarizations from −50 mV to +5 mV (duration, 75 ms; frequency, ~0·5 Hz). *A* shows that only a few I_{Ca} were able to trigger SR Ca^{2+} release. Two different current transients could be identified: two small ones (*) and a big one (●) which was composed of two components. The time course of the 'whole-line' ratio averaged from the entire line of the linescan image (*D*) is shown in *B*. *C* illustrates the time course of the ratio averaged from the top or the bottom part of the line (corresponding colour code in *D*). Different current and ratio transients averaged from the entire line or parts of the line were superimposed in *E*. *Ea* illustrates superimposed transients from the current transient with the two components (see *A*) while *Eb* shows the superimposed traces from the first SR Ca^{2+} release event (*A*). For a detailed description see the text.

transient. For Ca^{2+} release signals composed of two temporally separated release events (i.e. in the two ends of the cell) the bulk Ca^{2+} transient averaged from the entire cell should not match the current transient. On the other hand, the Ca^{2+} transients averaged from the two ends of the cell should resemble the time course of the two current components. To test this hypothesis we superimposed current (shown in black) and the local (red) and 'whole-line' (yellow) $[Ca^{2+}]$ revealed from the first small current component (see Fig. 4*E*). It is obvious that after amplitude normalization of all traces the time courses match each other. Therefore the time course of the global Ca^{2+} transient very much represents the time course of the local signal. Similar analysis performed for the W-shaped I_{NaCa} uncovered that the time course of the 'whole line' transient did not reflect that of the whole-cell membrane current (see Fig. 4*Ea*, left panel), but that each of the two components of the W-shaped membrane current were superimposable on the two isolated local Ca^{2+} transients averaged from the two ends of the cell (Fig. 4*Ea*, two right panels). Similar properties of the local Ca^{2+} transients averaged from the ends of the cell and the two components of the corresponding membrane current were found for all W-shaped I_{NaCa} signals obtained in this study ($n = 20$ in 5 cells).

Since the $[Ca^{2+}]$ at the wavefront had a similar amplitude during subcellular spreading (see Fig. 1), a given $[Ca^{2+}]$ at either end of the myocyte evoked a larger I_{NaCa} than in the middle of the cell. One possible explanation for this finding could be that the local surface-to-volume ratio for the particular cell segment is higher at the two ends than in the middle of the cell. Thus any Ca^{2+}-activated membrane current will have a higher amplitude at the two ends in response to a given $[Ca^{2+}]$.

In order to test this hypothesis we performed a simple simulation of a Ca^{2+} wave propagating through an elongated atrial myocyte.

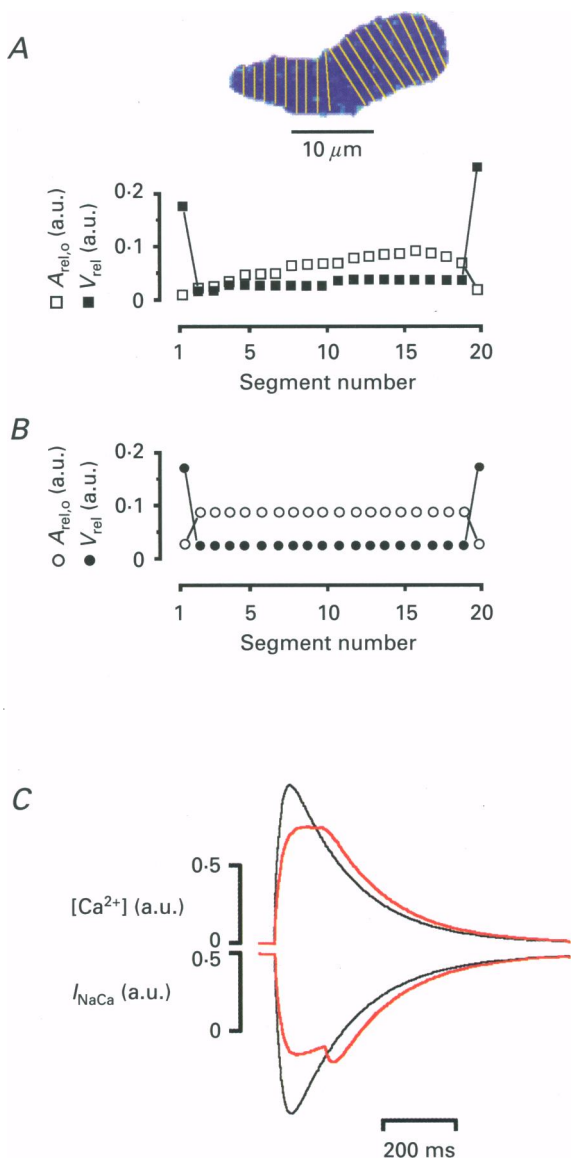

Figure 5. A simplified model for a propagating Ca^{2+} wave and the corresponding Ca^{2+}-activated membrane current (i.e. I_{NaCa})

The representative atrial myocyte used for all figures was divided into equally spaced (1 μm) slices as shown in the inset of *A*. Each slice is marked by yellow lines. The relative surface area ($A_{rel,o}$) and relative volume (V_{rel}) were calculated for each segment by assuming simple geometrical shapes (see text) and plotted against the segment number. A significant increase of the surface area-to-volume ratio was obvious for both cell ends. The surface area-to-volume ratio for each segment was simplified as shown in *B* and used for model calculations (as described in the text in greater detail). The time course for $[Ca^{2+}]$ (top traces in *C*) and I_{NaCa} (lower traces in *C*) were calculated for a homogeneous Ca^{2+} transient (shown in black) and for a Ca^{2+} wave propagating through the cell at a velocity of 50 μm s^{-1} (marked in red). The values for the parameters in eqn (3) used for this simulation were: $K_1 = 200\ s^{-1}$, $K_2 = 20\ s^{-1}$, $\beta = 1{\cdot}43$.

A model for the effect of Ca^{2+} wave propagation on the time course of I_{NaCa}

We divided the cell used for the results presented here into twenty 'slices' along its longitudinal axis (see Fig. 5*A*, inset). For each of these slices we calculated the relative membrane area ($A_{rel,o}$; membrane area of the particular 'slice' normalized to the membrane area of the entire cell) and relative volume (V_{rel}; volume of the 'slice' divided by the cell volume) by assuming simple geometrical shapes (e.g. cylinders, etc.). With the exception of the middle segment, all other segments were equally spaced (1 μm). A plot of $A_{rel,o}$ and V_{rel} against the segment number therefore characterized these values along the longitudinal axis of the cell. As shown in Fig. 5*A*, the $A_{rel,o}$ exhibits a steep increase when approaching the two cell ends while the relative volume seems to drop slightly. This U shape was characteristic for all cells analysed in this way ($n = 5$). In order to reduce the calculations for this model we simplified the relative areas and volumes as shown in Fig. 5*B*.

The cell geometry was reduced to a linear array of twenty equally spaced segments (x) each characterized by its relative volume and area. At both ends of the cell the relative area increased while the volume decreased. This model allows one to calculate the relative changes of the whole-cell Ca^{2+}-activated membrane current (e.g. I_{NaCa}) and the spatially averaged, whole-cell $[Ca^{2+}]$ by weighing the local $[Ca^{2+}]$ and current signals:

$$[Ca^{2+}]_{tot} = \sum_{x=1}^{n} (V_{rel,x}[Ca^{2+}]_x), \quad (1)$$

$$I_{NaCa} = -\alpha \sum_{x=1}^{n} ([Ca^{2+}]_x A_{rel,x}). \quad (2)$$

Here, $[Ca^{2+}]_{tot}$ represents the spatially averaged $[Ca^{2+}]$, n is the number of segments (20 in our model) and the index x assigns the local parameters and signals, while $V_{rel,x}$ indicates the relative volume of the x element (i.e. V_x/V_{tot}). The sign of α in eqn (2) solely accounts for the inward shift of I_{NaCa} upon a rise in $[Ca^{2+}]_i$ and α scales the current (this was set arbitrarily to 1 in all simulations and holds for unit conversions). The relative surface is indicated by $A_{rel,x}$ (i.e. A_x/A_{tot}). The change of $[Ca^{2+}]$ in each of the segments was calculated according to the eqn (3):

$$d[Ca^{2+}]_x/dt = (\beta K_1 e^{-K_1 t}) - (K_2 [Ca^{2+}]_x), \quad (3)$$

where K_1 and K_2 are time constants for the Ca^{2+} concentration increase and decrease, respectively. The variable β is a scaling factor.

This model further assumes that: (i) the Na^+–Ca^{2+} exchange molecules are homogeneously distributed over the plasma membrane; (ii) I_{NaCa} is a linear function of $[Ca^{2+}]$ (see Lipp *et al.* 1990 for atrial myocytes or Beuckelmann & Wier, 1989 for ventricular myocytes); (iii) the time course of the Ca^{2+} transient is the same in every segment; and (iv) the Ca^{2+} wave originates at one end of the cell and then propagates throughout the entire myocyte with a constant velocity (see Lipp & Niggli, 1993*b*) and a finite wavelength given by eqn (3). Propagation of the Ca^{2+} wave was simulated by simply delaying the onset of the Ca^{2+} transient for each segment by 20 ms resulting in a simulated propagation velocity of the wavefront of 50 $\mu m\ s^{-1}$, a value that is also seen in other cardiac preparations (see Fig. 1 and Lipp & Niggli, 1993*b*).

Figure 5*C* shows the result of two such simulations where the black traces correspond to a simulation with a homogeneous Ca^{2+} transient (i.e. the Ca^{2+} release was initiated simultaneously in every segment) and the traces in red resulted from a simulated Ca^{2+} wave. While the homogeneous Ca^{2+} release evoked a monophasic upstroke of both I_{NaCa} and the $[Ca^{2+}]$ transient, the simulated Ca^{2+} wave gave rise to a change in I_{NaCa} clearly composed of two components similar to those observed in the atrial myocytes (see Figs 2 and 4). We therefore conclude that the simplified assumption of a propagating Ca^{2+} wave was able to reflect basic characteristics of the current and $[Ca^{2+}]$ transients shown in atrial myocytes. Furthermore, the similarities between the recorded I_{NaCa} and those calculated with our model emphasized the suggested importance of the cell geometry (i.e. fractional membrane facing the Ca^{2+} transient) in determining the particular time course of the Ca^{2+}-activated membrane current (i.e. I_{NaCa}).

DISCUSSION

In the present paper we have examined the relationship between subcellular Ca^{2+} signals and the time course of a Ca^{2+}-dependent membrane current (i.e. I_{NaCa} that is linearly dependent on $[Ca^{2+}]$). In order to characterize the subcellular properties of intracellular Ca^{2+} signals we used a recently developed ratiometric confocal technique by combining the Ca^{2+}-sensitive indicators fluo-3 and Fura Red (Lipp & Niggli, 1993*a*).

I_{Ca} induced Ca^{2+} signalling in atrial myocytes

Previous studies without direct spatial information on the subcellular Ca^{2+} distribution in isolated guinea-pig atrial myocytes suggested that I_{Ca}-triggered SR Ca^{2+} release may initially be activated in a peripheral SR compartment underneath the cell membrane (Lipp, Pott, Callewaert & Carmeliet, 1993). Subsequent release was assumed to be triggered from a 'central' SR compartment. This notion was based on the simultaneous recording of I_{NaCa} and the bulk Ca^{2+} concentration (as calculated from the whole-cell indo-1 fluorescence). Later, evidence was presented for an additional role of this peripheral compartment in attenuating the I_{Ca}-mediated Ca^{2+} influx (Lipp *et al.* 1992). Similar observations with more direct visualization using confocal microscopy were described recently for field-stimulated, not voltage-clamped, atrial myocytes (Berlin, 1995; Hüser *et al.* 1996). Evidence was presented to show that in atrial cells SR Ca^{2+} release was initiated underneath the membrane and then invaded the interior of the myocyte in a 'wave-like' fashion.

This was attributed to the particular microarchitecture of mammalian atrial myocytes. In contrast to ventricular myocytes where the t-tubular system ensures homogeneous excitation of the entire cell (see e.g. Cheng *et al.* 1994) atrial myocytes lack such a system. Nevertheless Ca^{2+} gradients between subsarcolemmal compartments ('fuzzy space'; Lederer, Niggli & Hadley, 1990) were also proposed to exist in ventricular myocytes (see e.g. Trafford *et al.* 1995*a*).

I_{Ca} triggers Ca^{2+} waves in cultured atrial myocytes

During trains of I_{Ca}, SR Ca^{2+} release signals and accompanying I_{NaCa} with different spatiotemporal properties could be found. SR Ca^{2+} release that was apparently homogeneous within our limited temporal resolution (125 ms per image in the image mode or 25 ms per line in the linescan mode) was accompanied by an inward shift of I_{NaCa} with an initial phase that overlapped with I_{Ca}. In addition, mechanical contractions of the cell indicated that the principal steps of cardiac E–C coupling were operating despite the presence of a high concentration of the low-affinity Ca^{2+} buffer citrate. During trains of I_{Ca}, SR Ca^{2+} release was often spatially limited. These I_{Ca}-triggered local Ca^{2+} release events exhibited variable spreading inside the cell, i.e. either propagated through the entire cell (see Fig. 1*C*) or were restricted to one of the two sides of the elongated atrial myocytes (Fig. 3*C*). Both types of subcellular I_{Ca}-triggered Ca^{2+} waves were exclusively initiated at one of the two ends of the cell. This finding indicates that the partial uncoupling of Ca^{2+} release from Ca^{2+} influx caused by citrate may not be spatially homogeneous but instead was 'more effective' in the middle region of the elongated myocytes than at the two ends.

It has been shown previously that SR Ca^{2+} release in citrate-loaded atrial myocytes exhibits characteristics of a threshold phenomenon (Lipp *et al.* 1992; Callewaert, Sipido, Carmeliet, Pott & Lipp, 1995). During trains of I_{Ca}, Ca^{2+} influx was subthreshold while attenuation of the influx by the peripheral SR compartment gradually decreased until the SR Ca^{2+} release was finally triggered (see also Lipp *et al.* 1992). Because of the higher surface area per volume (relative surface area-to-volume ratio) at the two ends of the myocyte (compare with Fig. 5*A*) in comparison with the middle regions, Ca^{2+} influx per volume is relatively large in these regions. In consequence, the larger trigger signal for SR Ca^{2+} release and the higher Ca^{2+} loading state of the SR both increased the probability for Ca^{2+} release at the two ends. The distribution of the loading state in the longitudinal axis of the cell is thus similar to what was described recently for the perpendicular axis, i.e. the spreading of Ca^{2+} release from peripheral locations into the interior of cat atrial myocytes (Hüser *et al.* 1996). The latter can be interpreted in terms of (i) a higher trigger signal for the peripheral SR elements (i.e. preferential access) and (ii) a higher loading state of the SR and therefore a lower threshold for Ca^{2+} release. Both mechanisms are also pertinent for the triggering of I_{Ca}-induced Ca^{2+} waves in guinea-pig atrial myocytes at the two ends of the cell.

In guinea-pig atrial myocytes I_{Ca}-triggered Ca^{2+} release at the end of the cell may either spread throughout the entire cell or remain limited to one of the two halves of the myocyte. However, it should be noted here that entire or limited propagation was not a property of a particular cell (i.e. their individual geometry) but could be observed in all cells at a certain depolarization protocol. Similar transitions from subcellularly restricted propagation to spreading through the entire cell were also described recently for Ca^{2+} waves in adult rat ventricular myocytes (Trafford, Lipp, O'Neill, Niggli & Eisner, 1995*b*). In that study local activation of Ca^{2+} release was initiated by local application of caffeine through a pipette positioned near one end of a rat ventricular myocyte. Challenging the cell with caffeine at 2 mM Ca_o^{2+} resulted in a Ca^{2+} wave with limited subcellular propagation. Spreading of the Ca^{2+} wave through the entire cell could be obtained by increasing the $[Ca^{2+}]_o$ to 10 mM. This observation was explained by the increase of the positive feedback in the CICR mechanism when changing $[Ca^{2+}]_o$ from 2 to 10 mM which thereby most probably increased the luminal $[Ca^{2+}]$ in the SR that may modulate the gating properties of the SR Ca^{2+} release channels (for a review see Niggli & Lipp, 1995).

The degree of subcellular spreading of triggered Ca^{2+} waves depends on the duration of I_{Ca}

During trains of depolarizations that evoked long-lasting I_{Ca} (duration, $\geqslant$125 ms) Ca^{2+} waves propagated through the entire cell while shorter durations frequently resulted in Ca^{2+} waves with limited propagation. In citrate-loaded cardiac myocytes Ca^{2+}-dependent I_{Ca} inactivation is greatly reduced (Bechem & Pott, 1985; Lipp & Pott, 1991) and therefore the magnitude of Ca^{2+} influx is proportional to the duration of I_{Ca} even at durations $>$125 ms. Thus, variations in I_{Ca} duration (i.e. Ca^{2+} influx) will largely determine the loading of the SR and the positive feedback. We therefore conclude that the spatially limited propagation of the I_{Ca}-induced Ca^{2+} waves was most probably due to a lower degree of positive feedback in the CICR mechanism when using short I_{Ca} durations.

Moreover the observation of Ca^{2+} waves with propagation failures in the middle of the elongated cell suggested that the positive feedback exhibited by 'middle' SR compartments was lower than at the ends. The relative surface area-to-volume ratio profile shown in Fig. 5 may therefore indirectly represent the distribution of positive feedback in CICR along the longitudinal cell axis. This conclusion further supports our view of the SR as a 3-dimensional network of functionally separated SR elements (for a recent review see Niggli & Lipp, 1995) and the possibility of the coexistence of SR elements with different degrees of positive feedback.

The time course of I_{NaCa} is dependent on the spatiotemporal properties of the underlying subcellular Ca^{2+} transient

During trains of I_{Ca}, changes of I_{NaCa} were observed with initial phases that were either fused with I_{Ca} or temporally

well separated from I_{Ca}. Those changes of I_{NaCa} with a temporal separation from I_{Ca} exhibited a time course composed of two distinct initial phases (see Figs 1 and 2) or two small components (see Fig. 4). Similar observations have been described (Lipp *et al.* 1990; Budde *et al.* 1991) and were interpreted in terms of Ca^{2+} release from a peripheral and central SR compartment. In contrast, the direct visualization of subcellular SR Ca^{2+} release by ratiometric confocal microscopy in the present study suggested another interpretation. Propagation of Ca^{2+} waves along the longitudinal axis of the myocytes gave rise to I_{NaCa} exhibiting two current components. Therefore the temporal separation of the two I_{NaCa} components was found to depend on the volume fraction of the myocyte occupied by the Ca^{2+} wave and the individual cell geometry in terms of the longitudinal surface area-to-volume ratio (see Fig. 5). At the two ends of the myocyte a particular $[Ca^{2+}]$ was facing a larger membrane fraction than in the middle regions. SR Ca^{2+} release with propagation failures evoked changes in I_{NaCa} that could be identified as the 'small component' described elsewhere (Lipp *et al.* 1990; Budde *et al.* 1991).

In adult rat ventricular myocytes the analysis of the relation between I_{NaCa} and $[Ca^{2+}]_i$ by means of video microscopy indicated similar non-linearities (Trafford *et al.* 1995*a*) to those found in atrial myocytes (Lipp *et al.* 1990). The different interpretations of the present results obtained with confocal microscopy and those by Trafford *et al.* may be due to the inherently lower spatial resolution offered by the video microscopy technique. This drawback usually does not allow for an easy identification of Ca^{2+} waves travelling in the z-direction (both partially or exclusively). The spread of a Ca^{2+} wave in the z-axis may show up as a stationary or slowly propagating Ca^{2+} wave, making it difficult to evaluate the membrane area that is affected by the elevated $[Ca^{2+}]_i$. But this membrane area, as pointed out in this paper, is a critical parameter determining the precise I_{NaCa} *vs.* $[Ca^{2+}]_i$ relation. Therefore, the proposed subsarcolemmal gradients of $[Ca^{2+}]_i$ are not required to model the time course of I_{NaCa} during triggered Ca^{2+} waves in atrial myocytes.

A geometrical model is able to reproduce the time course of I_{NaCa} in response to Ca^{2+} transients with different subcellular properties

A mathematical model incorporating linear propagation of a Ca^{2+} wave through an elongated atrial myocyte was able to reproduce the experimental results. Therefore, we conclude that the time course of I_{NaCa} is determined to a large extent by (i) the subcellular properties of SR Ca^{2+} release and (ii) the individual cell geometry of the particular myocyte. We further propose that the subcellular property of the Ca^{2+} signal and the cell geometry are important determinants not only for the time course of I_{NaCa} but also for every Ca^{2+}-activated membrane current (e.g. the Ca^{2+}-activated Cl^- current). Consequently, interpretation of Ca^{2+}-activated membrane currents in terms of the subcellular properties of the underlying Ca^{2+} signals may be difficult.

In summary we were able to identify I_{Ca}-triggered Ca^{2+} waves with different subcellular spreading in single atrial myocytes from guinea-pigs. The magnitude of the local Ca^{2+} influx is an important determinant of the positive feedback in the CICR mechanism produced by the single SR element in the subcellular 3-dimensional SR network. Local differences in this positive feedback may result from the local surface area-to-volume ratio and modulate the subcellular propagation patterns of I_{Ca}-induced Ca^{2+} waves. The microscopic properties of the Ca^{2+} waves in turn determine the particular time course of Ca^{2+}-modulated membrane currents (e.g. I_{NaCa}).

Bechem, M., Pieper, F. & Pott, L. (1985). Guinea-pig atrial cardioballs. *Basic Research in Cardiology* **80**, 19–22.

Bechem, M. & Pott, L. (1985). Removal of Ca current inactivation in dialyzed guinea-pig atrial cardioballs by Ca chelators. *Pflügers Archiv* **404**, 10–20.

Berlin, J. B. (1995). Spatiotemporal changes of Ca^{2+} during electrically evoked contractions in atrial and ventricular cells. *American Journal of Physiology* **269**, H1165–1170.

Beuckelmann, D. J. & Wier, W. G. (1989). Sodium–calcium exchange in guinea-pig cardiac cells: exchange current and changes in intracellular Ca^{2+}. *Journal of Physiology* **414**, 499–520.

Budde, T., Lipp, P. & Pott, L. (1991). Measurement of Ca^{2+}-release-dependent inward current reveals two distinct components of Ca^{2+}-release from sarcoplasmic reticulum in guinea-pig atrial myocytes. *Pflügers Archiv* **417**, 638–644.

Callewaert, G. (1992). Excitation–contraction coupling in mammalian cardiac cells. *Cardiovascular Research* **26**, 923–932.

Callewaert, G., Sipido, K. R., Carmeliet, E., Pott, L. & Lipp, P. (1995). Intracellular citrate induces regenerative calcium release from sarcoplasmic reticulum in guinea-pig atrial myocytes. *Pflügers Archiv* **429**, 797–804.

Cheng, H., Lederer, W. J. & Cannell, M. B. (1994). Propagation of excitation–contraction coupling into ventricular myocytes. *Pflügers Archiv* **428**, 415–417.

Hüser, J., Lipp, P., Pott, L. & Niggli, E. (1994). Cell geometry determines subcellular calcium signaling in single atrial myocytes. *Biophysical Journal* **66**, A94.

Hüser, J., Lipsius, S. L. & Blatter, L. A. (1996). Calcium gradients during excitation–contraction coupling in cat atrial myocytes. *Journal of Physiology* **494**, 641–651.

Leblanc, N. & Hume, J. R. (1990). Sodium current induced release of calcium from cardiac sarcoplasmic reticulum. *Science* **248**, 372–376.

Lederer, W. J., Niggli, E. & Hadley, R. W. (1990). Sodium–calcium exchange in excitable cells: Fuzzy space. *Science* **248**, 283.

Lipp, P. & Niggli, E. (1993*a*). Ratiometric confocal Ca^{2+} measurements with visible wavelength indicators in isolated cardiac myocytes. *Cell Calcium* **14**, 359–372.

Lipp, P. & Niggli, E. (1993*b*). Microscopic spiral-waves reveal positive feedback in subcellular calcium signaling. *Biophysical Journal* **65**, 2272–2276.

Lipp, P. & Niggli, E. (1994*a*). Sodium current-induced calcium signals in isolated guinea-pig ventricular myocytes. *Journal of Physiology* **474**, 439–446.

Lipp, P. & Niggli, E. (1994*b*). Modulation of Ca^{2+} release in neonatal cultured rat cardiac myocytes: Insight from subcellular release patterns revealed by confocal microscopy. *Circulation Research* **74**, 979–990.

Lipp, P. & Pott, L. (1991). Effect of intracellular Ca^{2+}-chelating compounds on inward currents caused by Ca^{2+} release from sarcoplasmic reticulum in guinea-pig atrial myocytes. *Pflügers Archiv* **419**, 296–303.

Lipp, P., Pott, L., Callewaert, G. & Carmeliet, E. (1990). Simultaneous recording of indo-1 fluorescence and Na^+/Ca^{2+} exchange current reveals two components of Ca^{2+}-release from sarcoplasmic reticulum of cardiac atrial myocytes. *FEBS Letters* **275**, 181–184.

Lipp, P., Pott, L., Callewaert, G. & Carmeliet, E. (1992). Calcium transients caused by calcium entry are influenced by the sarcoplasmic reticulum in guinea-pig atrial myocytes. *Journal of Physiology* **454**, 321–338.

Niggli, E. & Lipp, P. (1993). Subcellular restricted spaces: significance in cell signaling and excitation–contraction coupling. *Journal of Muscle Research and Cell Motility* **14**, 288–291.

Niggli, E. & Lipp, P. (1995). Subcellular features of calcium signalling in heart muscle: what do we learn? *Cardiovascular Research* **29**, 441–448.

Pott, L. & Mechmann, A. (1990). Large-conductance ion channel measured by whole-cell voltage clamp in single cardiac cells: modulation by β-adrenergic stimulation and inhibition by octanol. *Pflügers Archiv* **117**, 189–199.

Sham, J. S. K., Cleemann, L. & Morad, M. (1992). Gating of cardiac Ca^{2+} release channel: The role of Na^+ current and Na^+–Ca^{2+} exchange. *Science* **255**, 850–853.

Sommer, J. R. & Jennings, R. B. (1986). Ultrastructure of cardiac muscle. In *The Heart and Cardiovascular System*, ed. Fozzard, H. A., Haber, E., Jennings, R. B., Katz, A. M. & Morgan, H. E., pp. 61–100. Raven Press, New York.

Takamatsu, T. & Wier, W. G. (1990). High temporal resolution video imaging of intracellular calcium. *Cell Calcium* **11**, 111–120.

Trafford, A. W., Diaz, M. E., O'Neill, S. C. & Eisner, D. A. (1995*a*). Comparison of subsarcolemmal and bulk calcium concentration during spontaneous calcium release in rat ventricular myocytes. *Journal of Physiology* **488**, 577–586.

Trafford, A. W., Lipp, P., O'Neill, S. C., Niggli, E. & Eisner, D. A. (1995*b*). Propagating calcium waves initiated by local caffeine application in rat ventricular myocytes. *Journal of Physiology* **489**, 319–326.

Acknowledgements

The authors thank Drs S. L. Lipsius and L. A. Blatter for critical discussion and helpful comments on an earlier version of this manuscript, and Dr H. G. Glitsch for continuous support. This work was supported by the Swiss National Foundation.

Author's present address

J. Hüser: Loyola University Chicago, Department of Physiology, 2160 S. First Avenue, Maywood, IL 60153, USA.

Received 5 July 1996; accepted 13 September 1996.